Kicked rotor with attosecond pulse train

D.R.Mašović

Vinča Institute of Nuclear Sciences
Laboratory for Theoretical and Condensed Matter Physics, 11001 Belgrade, P.O.Box 522, Serbia
dmasovic@vinca.rs
dragmasovic@gmail.com

Abstract

The kicked rotor is one of the basic models in connection with chaos and quantum chaos. A possible application of an attosecond pulse train as a kicking field in the kicked rotor is theoretically examined for the first time. This version of the kicked rotor is denoted as an *atto*-kicked rotor. It seems to be the most realistic version of the kicked rotor because it takes into account the real form of the kicking field as it appears in the experiments. The *atto*-kicked rotor is investigated from the classical and the quantum aspects. In the classical case, a new map instead of the Chirikov standard map is proposed. It may be useful in appropriate experiments with the classical chaos. In the quantum case, the *atto*-kicked rotor gives satisfactory results. Phenomena such as dynamical localization and quantum resonances appear in the undisturbed form. It may be also used for examining the influence of the quantum effects on classical chaos and diffusion.

KEYWORDS:
kicked rotor, chaos, quantum chaos, attosecond pulse train, dynamical localization, quantum resonance

PACS numbers: 05.45.Pq , 42.65.Ky , 05.45.Mt , 72.15.Rn

I. Introduction

Periodically driven systems, classical and quantum, usually represented by the kicked rotor (KR) have been extensively studied in the recent past in connection with chaos and quantum chaos, see for example [1 , 2 , 3 , 4]. One of the main discoveries obtained on the basis of this very popular model for quantum chaos is that the quantum effects tend to suppress the classical chaos and diffusion by a mechanism that is similar to the Anderson localization in disordered solids [5]. For large kicks strengths the effects of quantum resonance and dynamical localization (non-resonant effect) are established. Further investigations are expanded towards real systems such as, for example, hydrogen atom in a microwave field [6]. Theoretical examinations also include electron spin influence in the framework of the appropriate quantum KR model [7 , 8 , 9 , 10]. One reason that the KR is an especially interesting problem is that it can be realized experimentally. Such experimental research exists in our time, too. Raizen and coworkers [11] used a system of ultracold atoms interacting with a pulsed standing light wave in the experiment. Thus, the first realization of the quantum KR known as atom-optics KR was achieved. That system has become the standard setup for observing the effects of quantum resonance and dynamical localization. Further, the quasi periodic quantum KR as a version of atom-optics KR is experimentally realized [12]. In particular, the effects of phase noise i.e. the influence of sinusoidal phase modulation on both the resonant and non-resonant dynamics of the quantum KR was examined theoretically and experimentally in the Auckland group [13]. Special interest in the quantum KR exists in molecular physics. Rotation of diatomic molecules is the most basic version of quantum rotors. Therefore, interaction of diatomic molecules with a periodic sequence of ultrashort laser pulses i.e. laser induced molecular rotation and alignment are in the focus of research. In this way the problem of a KR is revisited in order to find new mechanisms for laser control of molecular rotational wave packets. The effects of quantum resonance and dynamical localization are registered experimentally [14, 15]. The appropriate theoretical investigations based on KR follow these experiments [16].

High-order harmonic generation (HHG) refers to the problem of generating high-frequency pulses from low-frequency one. In general, harmonic generation is a feature of driven nonlinear systems. Specially, when a very intense laser pulse is focused on an atomic gas, strong nonlinear laser-atom interactions can lead to the generation of very high harmonics of the optical frequency of the pulse [17 , 18]. It is an extreme form of nonlinear frequency conversion and only odd harmonics of the incident radiation frequency are emitted. The most significant manifestation of this behavior is existence of a plateau in the harmonics spectrum in which harmonics up to the characteristic cutoff have fairly uniform intensity. Thus, HHG has recently become a base for attosecond pulses production [19 , 20 , 21].

HHG is a highly nonlinear phenomenon and it can be understood on the basis of the three-step model [22 , 23]. In the first step, the ionization of an atom by a strong, linearly polarized laser field occurs. During the second step, thus released free electron is accelerated away from the ion core. When the laser electric field changes its sign the electron returns and collides with the core. In the last step, the ionized electron can recombine with its parent ion. This results in a high-order harmonic emission. It is

a generally accepted and proven model for HHG in atomic gases.

However, this is not necessarily the only way for HHG. In Ref.[24] a special type of confinement is suggested for simulating the interaction of an atom with the surrounding ones in a high pressure hydrogen atomic gas. Then, in addition to the laser pulse, the kicking electric field i.e. the impulsive train, is added at the moments when the ionization probability is at a maximum. Thus, the electron kinetic energy is drastically increased, and as a consequence of the dynamic Stark shifts in the energy spectrum, an unusual electron recombination can happen. As a result of such recombination, a very high order of harmonics appears. Further, in [25] the interaction of the kicking laser electric field with a single electron cylindrical quantum dot without and in the presence of an external magnetic field is considered. It is shown that the kicking field generates harmonics of a very high-order. This is based on the fact that during the kick the electron energy is increased and it is associated with the pronounced quantum-confined Stark effect in the energy spectrum. The occurrence of these harmonics is a consequence of the electron transition to the inner shells. In addition, application of the kicking field for example, in the solid state physics is considered in Ref.[26]. We note that the problem of underlying classical dynamic, chaotic and regular, and its influence on HHG is investigated in Ref.[27]. Considerations are first from the quantum and then from the classical aspect.

It should be pointed out that there are two goals for the attosecond pulse synthesis from HHG. One is the generation of isolated attosecond pulse utilizing HHG with a few-cycle driving pulse.This implies a continuous harmonic spectrum in and over the cutoff frequency. In this case the emission of cutoff harmonics is temporarily confined into one single burst. The other goal is the formation of attosecond pulse train (APT) from the broad plateau spectrum. It has been experimentally demonstrated that a train of pulses as short as a few hundred attoseconds is obtained when several odd harmonics of an intense, infrared, linearly polarized laser field are combined in a phase-locked manner [28]. The short duration of the individual pulses in the train and their periodicity make the APT convenient for kicking field.

Here, we examine theoretically realization of KR with APT. The experimental applications, specially in molecular physics are kept in mind. The organization of the rest of the paper is as follows. In Sec.II the APT is given. In Sec.III classical KR and in Sec.IV quantum KR are analyzed. The conclusions are given in Sec.V .

II. APT

APT is proposed theoretically in Ref.[29]. It is based on experimentally obtained HHG by the interaction of a strong laser field with angular frequency ω=0.057 a.u. ($\mid e \mid = m_e = \hbar = 1$) with a gaseous sample. Then, harmonics from the plateau spectrum are almost phase-locked. By superposing sets of high harmonics, it is possible to produce APT. Such an electric field can be approximated

(monochromatic limit) as

$$E_h(t) = \frac{E_h^0}{\bar{\sigma}(t)} \sum_{q=2k_0+1}^{2k_1+1} \sin(q\omega t - q\varphi) \quad , \tag{2.1}$$

where E_h^0 is the amplitude of the field and $\bar{\sigma}(t)$ is the train temporal envelope, which will be taken as $\bar{\sigma}$=1 [30]. In (2.1)

$$\varphi = \omega t_d \quad , \tag{2.2}$$

where t_d is the time delay. Note that such a train has a time delay with respect to the driven field. For φ=0 this is an idealized train. Here, we will always assume φ=0.75π. In Eq.(2.1) the sum is over five odd harmonics 11-19 and $2k_0+1$ and $2k_1+1$ are the minimal and the maximal harmonics order, respectively. From Ref.[29] the APT peak intensity is $10^{13}\frac{W}{cm^2}$. It should be emphasized that physically $E_h(t)$ corresponds to an infinitely long train of pulses suitable for KR considerations.

It can be also approximately assumed that $E_h(t)$ is periodic function with period $T_0 = \frac{\pi}{\omega} = \frac{T}{2}$, where T is the period of driven field, see Fig.1. This is in agreement with [31]. The duration of the individual pulses in the train is $\bar{\varepsilon} \sim 400$ attoseconds.

III. Classical KR

A simple KR model is proposed in Ref.[8]. The model is suitable for physical performance of KR. An electron in the impenetrable ring with radius r located in the $x0y$ plane simulates the rotor while the kicking electric field is along x axis. Such a KR model can be treated in the classical and in the quantum ways. In the classical case the time-dependent Hamiltonian is

$$H = \frac{p^2}{2I} + \bar{k}\cos\theta \cdot \Delta(t) \quad , \tag{3.1}$$

where $p = m_e r^2\dot{\theta}$ is the angular momentum, θ is angle with respect to the x axis, $I = m_e r^2$ is the moment of inertia and parameter $\bar{k} =\mid e \mid \bar{E}r$, where $\bar{E}$ is the amplitude of the kicking electric field. $\Delta(t)$ in (3.1) is given as

$$\Delta(t) = \sum_{n=-\infty}^{\infty} \delta(\frac{t}{T_0} - n) \quad . \tag{3.2}$$

This model is referred to as δ-KR . It is the standard model in most of KR considerations. In the limit of arbitrary short pulses, the pulse function is usually replaced by Dirac delta function $\delta(t)$. However, we emphasized that in Ref.[16] Gaussian pulses are used. This case will be also considered

$$\Delta(t) = \frac{1}{\sigma\sqrt{2\pi}} \sum_{n=-\infty}^{\infty} e^{-\frac{\left(\frac{t}{T_0} - n\right)^2}{2\sigma^2}} \quad , \tag{3.3}$$

where σ is a measure for the pulse duration. It will be denoted as the σ-KR model.

Definitely APT from (2.1) implies

$$\Delta(t) = \begin{cases} \sum_{q=2k_0+1}^{2k_1+1} \sin(tq\omega T_0 - q\omega t_0 - q\varphi) \ , & n - \frac{\bar{\varepsilon}}{2T_0} \leqslant t \leqslant n + \frac{\bar{\varepsilon}}{2T_0} \\ & n \in (-\infty, +\infty) \\ 0 \ , \quad \text{otherwise} \end{cases} \tag{3.4}$$

The noise-oscillations between pulses are here neglected. Thus, it will be the *atto*-KR . It may be the most realistic version of KR since it also takes into account the oscillations within the pulse as they appear in the experiments.

Rotational dynamics of the δ-KR is examined with the Chirikov standard map [4 , 32]. This is one of the most important maps in the conservative chaos theory. It is used, besides other applications, to estimate the onset of chaos in the δ-KR . The map is given by the following set of equations

$$P_{n+1} - P_n = \mathrm{K} \sin\theta_n \tag{3.5}$$

$$\theta_{n+1} - \theta_n = P_{n+1} \tag{3.6}$$

where P and K are dimensionless angular momentum and control parameter, respectively. Eqs. (3.5) and (3.6) are derived from the Hamiltonian (3.1) assuming (3.2). Due to the periodicity of $\sin\theta_n$ in (3.5) the dynamics is usually considered on a torus (by taking $\theta, P \mod 2\pi$). The map has been thoroughly examined and it is just enough to note that the spread of chaos is associated with increased values of parameter K .

In [16] the authors refer to the Cryan et al [33] experiment where a laser pulse train was used to induce a strong nitrogen alignment. Pulses of 50 fs 800 nm at 1 kHz repetition rate were applied. The authors further call for an experimental application in laser-kicked molecules and observing phenomena of quantum δ-KR . For such a pulse train $\frac{\bar{\varepsilon}}{T_0}$ is as a small parameter and the classically considered problem essentially on the basis of σ-KR is reduced to the Chirikov standard map. In general, a pulse train is not necessary as previous, for example APT in (2.1) where $\frac{\bar{\varepsilon}}{T_0}$ is not a small parameter. Then the possibility of applying σ-KR in this approach, that is approximate APT pulses with Gaussian ones, may also be considered. We emphasize that in this case σ-KR can only in an approximation be brought down to the Chirikov standard map.

The situation is something different for *atto*-KR . Here, the limit $\frac{\bar{\varepsilon}}{T_0} \to 0$ is not considered at all as unrealistic, see Sec.II . The ratio of $\frac{\bar{\varepsilon}}{T_0}$ is not a small parameter and definitely, the *atto*-KR can not be reduced to the Chirikov standard map. Therefore, an alternative and approximate map is proposed here

$$P_{n+1} - P_n = \bar{K} F_n \sin\theta_n \tag{3.7}$$

$$\theta_{n+1} - \theta_n = S P_{n+1} \tag{3.8}$$

where $\bar{K}$ is a new control parameter,

$$S = \frac{T_0 - \bar{\varepsilon}}{T_0} \quad , \tag{3.9}$$

and

$$F_n = \frac{2}{\pi} \sum_{q=2k_0+1}^{2k_1+1} \frac{1}{q} \sin(nq\omega T_0 - q\omega t_0 - q\varphi) \sin \frac{\bar{\varepsilon}}{2} q\omega \quad . \tag{3.10}$$

The map is tested for the corresponding values of parameter $\bar{K}$ assuming θ, P on a torus, Figs. 2-5. The spread of chaos is clearly shown with increased values of parameter $\bar{K}$. In particular, it is well known that the classical δ-KR assuming the fully developed chaos shows a diffusive growth of energy i.e. the average kinetic energy (or rotational energy) is given as

$$< E_n > \sim \frac{1}{4} K^2 n \quad . \tag{3.11}$$

In order to check our map reliability we have calculated kinetic energy for $\bar{K}$= 500 . The result is shown in Fig.6. Linear growth on average is clearly visible but it is of course different from (3.11).

Map (3.7)-(3.8) may be useful for experiments with classical chaos and possible application of APT .

IV. Quantum KR

The Hamiltonian for quantum KR can be written

$$H = \frac{\tau}{2}p^2 + k\cos\theta \cdot \Delta(t) \quad , \tag{4.1}$$

where τ and k are dimensionless parameters. In this form (4.1) is derived from (3.1). It is also assumed in $\{\theta\}$ representation for operator $p^2 = -\frac{\partial^2}{\partial\theta^2}$. Due to periodicity in time

$$H(t) = H(t+1) \quad . \tag{4.2}$$

Then, the problem is reduced to solve time-dependent Schrödinger equation

$$i\frac{\partial\Psi}{\partial t} = H\Psi \quad , \tag{4.3}$$

where $\Psi \equiv \Psi(\theta, t)$. Supposing quantum δ-KR and (3.2), the solution for one period is

$$\Psi^-(\theta, t+1) = U\Psi^-(\theta, t) = e^{-\frac{\tau}{2}p^2}e^{-ik\cos\theta}\Psi^-(\theta, t) \quad , \tag{4.4}$$

where U is the evolution operator.The first factor on the right in (4.4) describes the evolution of the rotor between the kicks, and the second factor describes the effect of the kick. From now on Ψ^- and Ψ^+ denote the state of the system at time just before and just after the kick, respectively. Since the Hamiltonian is periodic in time quasienergy Ω is introduced and the wave function must be in the Bloch-Floquet form

$$\Psi^-_\Omega(\theta, t) = e^{-i\Omega t}u^-_\Omega(\theta, t) \quad , \tag{4.5}$$

where is

$$u^-_\Omega(\theta, t) = u^-_\Omega(\theta, t+1) \quad , \tag{4.6}$$

and

$$u^-_\Omega(\theta, t) = \frac{1}{\sqrt{2\pi}}\sum_{m=-N}^{N} u^-_m e^{im\theta} \quad , \tag{4.7}$$

with

$$u^-_m \equiv u^-_{m\Omega}(t) = u^-_{m\Omega}(t+1) \quad . \tag{4.8}$$

It is also known that

$$[\ \mathrm{I}\ ,\ U\ ] = 0 \quad , \tag{4.9}$$

where I is parity operator. Thus, $\Psi^-_\Omega(\theta, t)$ (and $\Psi^+_\Omega(\theta, t)$) states in (4.5) can be either even or odd. For example, from a physical point of view for the model mentioned at the beginning of Sec.III the parity operator is : $\mathrm{I} = R_x$ (rotation by π , about the x axis) or $\mathrm{I} = S_y$ (reflection in the plane normal to $\vec{i}_y$) .

For quantum σ-KR the evolution operator instead of the one in (4.4) is

$$U = e^{-i\frac{\tau}{2}\left(1-\frac{\bar{\varepsilon}}{T_0}\right)p^2} e^{-i\frac{\tau}{2}\frac{\bar{\varepsilon}}{T_0}p^2 - ik\cos\theta} \quad , \tag{4.10}$$

where is

$$e^{-i\frac{\tau}{2}\frac{\bar{\varepsilon}}{T_0}p^2 - ik\cos\theta} = e^{-ik\cos\theta - i\frac{\tau}{2}\frac{\bar{\varepsilon}}{T_0}p^2} \tag{4.11}$$

and unitarity is conserved. Here, $\frac{\bar{\varepsilon}}{T_0}$ will not be treated as a small parameter. This is an important assumption for the eventual application of σ-KR in the APT approach. We introduce shorter notation for the operators

$$A = \frac{\tau}{2}\frac{\bar{\varepsilon}}{T_0}p^2 \quad \text{and} \quad B = k\cos\theta \quad .$$

Those are non-commuting operators and the second factor in (4.10) in the form $e^{-i(A+B)}$ is the main problem. It now describes the kick effect.Then, the following relation holds

$$e^{-i(A+B)} = \left[e^{-i(\frac{A}{M}+\frac{B}{M})}\right]^M \quad , \tag{4.12}$$

where $M \to \infty$. Further, we can apply the Trotter product formula [34]

$$e^{-i(\frac{A}{M}+\frac{B}{M})} = e^{-i\frac{A}{M}} e^{-i\frac{B}{M}} + O(\frac{1}{M^2}) \quad , \tag{4.13}$$

where is

$$O(\frac{1}{M^2}) \ \sim \ \frac{e^{-i\frac{A}{M}} e^{-i\frac{B}{M}}}{M^2} \ \ \frac{\tau}{4}\frac{\bar{\varepsilon}}{T_0}k(\cos\theta + i2\sin\theta\cdot p) \tag{4.14}$$

in the operator form, where $p = -i\frac{\partial}{\partial\theta}$ is the angular momentum. In particular, the appropriate matrix elements are now calculated

$$< m \mid e^{-i(A+B)} \mid s >= \sum_{l_1=-N}^{N}\sum_{l_2=-N}^{N}\cdots\sum_{l_{M-1}=-N}^{N} < m \mid e^{-i\frac{A}{M}} e^{-i\frac{B}{M}} + O(\frac{1}{M^2}) \mid l_1 >$$

$$< l_1 \mid e^{-i\frac{A}{M}} e^{-i\frac{B}{M}} + O(\frac{1}{M^2}) \mid l_2 >$$

$$\cdot$$

$$\cdot$$

$$\cdot$$

$$< l_{M-1} \mid e^{-i\frac{A}{M}} e^{-i\frac{B}{M}} + O(\frac{1}{M^2}) \mid s >=$$

$$= \sum_{l_1=-N}^{N}\sum_{l_2=-N}^{N}\cdots\sum_{l_{M-1}=-N}^{N} < m \mid e^{-i\frac{A}{M}} e^{-i\frac{B}{M}} \mid l_1 >$$

$$< l_1 \mid e^{-i\frac{A}{M}} e^{-i\frac{B}{M}} \mid l_2 >$$

$$
\begin{aligned}
&\cdot \\
&\cdot \\
&\cdot \\
&< l_{M-1} \mid e^{-i\frac{A}{M}} e^{-i\frac{B}{M}} \mid s > \ + \\
&+ \ M(2N+1)O(\frac{1}{M^2}) \quad . \qquad (4.15)
\end{aligned}
$$

From (4.15) it follows

$$
\begin{aligned}
&< m \mid e^{-i(A+B)} \mid s >= \\
&= i^{m-s} \sum_{l_1=-N}^{N} \sum_{l_2=-N}^{N} \cdots \sum_{l_{M-1}=-N}^{N} e^{-i\frac{\tau}{2}\frac{\varepsilon}{T_0}\frac{m^2+l_1^2+\cdots+l_{M-1}^2}{M}} \ . \\
&\cdot \ J_{l_1-m}(\frac{k}{M}) J_{l_2-l_1}(\frac{k}{M}) \cdots J_{s-l_{M-1}}(\frac{k}{M}) \ + \ (2N+1)O(\frac{1}{M}) \quad , \qquad (4.16)
\end{aligned}
$$

where J are Bessel functions of the first kind. For a great values of M , $\frac{k}{M}$ in J is very small and we have $(2N+1) \sim 1$ in (4.16) .

Further simplification for matrix elements can be obtained by analysis

$$
\begin{aligned}
&\sum_{l_1=-N}^{N} \sum_{l_2=-N}^{N} \cdots \sum_{l_{M-1}=-N}^{N} e^{-i\frac{\tau}{2}\frac{\varepsilon}{T_0}\frac{m^2+l_1^2+\cdots l_{M-1}^2}{M}} \ . \\
&\cdot \ J_{l_1-m}(\frac{k}{M}) J_{l_2-l_1}(\frac{k}{M}) \cdots J_{s-l_{M-1}}(\frac{k}{M}) \qquad (4.17)
\end{aligned}
$$

in (4.16) for $k \to 0$ when $J_{s-m}(k) \to \delta_{s,m}$. Then,

$$
J_{l_1-m}(\frac{k}{M}) J_{l_2-l_1}(\frac{k}{M}) \cdots J_{s-l_{M-1}}(\frac{k}{M}) \ = \ \delta_{l_1,m}\delta_{l_2,l_1}\cdots\delta_{s,l_{M-1}} \ = \ \delta_{s,m} \qquad (4.18)
$$

and

$$
\frac{m^2+l_1^2+\cdots+l_{M-1}^2}{M} \ = \ s^2 \quad . \qquad (4.19)
$$

Thus, it is proved in the limit $k \to 0$ that the expression in (4.17) can be reduced to the form which exists in δ-KR

$$
e^{-i\frac{\tau}{2}\frac{\varepsilon}{T_0}s^2} J_{s-m}(k) \quad . \qquad (4.20)
$$

Then, the main problem seems solved

$$
< m \mid e^{-i(A+B)} \mid s >=< m \mid e^{-iA} e^{-iB} \mid s > + O(\frac{1}{M}) \quad , \qquad (4.21)
$$

where $M \to \infty$. Finally, after the appropriate calculation the well known quantum δ-KR eigenvalue problem approximately appears with respect to the estimated accuracy in (4.21). It means that the

quantum σ-KR is also suitable to simulate the quantum δ-KR in the case when $\frac{\bar{\varepsilon}}{T_0}$ is not a small parameter.

Further, the evolution operator for the quantum *atto*-KR in (4.4) is

$$U = e^{-i\frac{\tau}{2}\left(1-\frac{\bar{\varepsilon}}{T_0}\right)p^2} e^{-i\frac{\tau}{2}\frac{\bar{\varepsilon}}{T_0}p^2 + i\bar{S}k\cos\theta} \quad , \tag{4.22}$$

where

$$\bar{S} = \frac{T}{\pi T_0} \sum_{q=2k_0+1}^{2k_1+1} \frac{1}{q} \sin(q\omega t_0 + q\varphi) \sin\frac{\bar{\varepsilon}}{2} q\omega \; = 0.012682468 \quad . \tag{4.23}$$

In the same way as before the quantum δ-KR eigenvalue problem is obtained with the same accuracy as previously

$$\sum_{l=-N}^{N} \left[\; i^{m-l} J_{m-l}(\tilde{k}) e^{-i\frac{\tau}{2}l^2} - e^{-i\Omega}\delta_{ml} \; \right] u_l^+ \simeq 0 \quad , \tag{4.24}$$

where $\tilde{k} = \bar{S}k$. It is an important result. All phenomena of the quantum δ-KR persist in the *atto* case, too, and the only change is $k \to \tilde{k}$.

We note that the quantum δ-KR eigenvalue problem can be also considered by using sets of symmetry adapted basis functions, particularly for even and particularly for odd states. Thus, for example, for odd states the appropriate eigenvalue problem is

$$\sum_{l=1}^{N} \left(\; \bar{U}_{ml} - e^{-i\Omega}\delta_{ml} \; \right) v_l^- \simeq 0 \quad , \tag{4.25}$$

where are

$$\bar{U}_{ml} = < m \mid U \mid l > - < m \mid U \mid -l > \tag{4.26}$$

and

$$v_l^- = \sqrt{2} u_l^- \quad . \tag{4.27}$$

By solving (4.24) for large $\tilde{k}$ quantum δ-KR phenomena can be seen. When $\frac{\tau}{4\pi}$ is an irrational number, dynamical localization appears. It is an exponential localization in angular momentum space similar to the Anderson localization in disordered solid [5]. The example is shown in Fig.7 . The exponential drop is clearly visible. In addition, in Fig.8 another example obtained by solving (4.25) is given. For values $\frac{\tau}{4\pi} = \frac{p}{q}$ the quantum resonances appear. In Fig.9 such an example is presented.

Next, we consider influence of noise-oscillations between pulses in quantum *atto*-KR. Therefore, we assume approximate periodicity in the noise-oscillations with period T_0 (see Fig.1) so that (4.2) is still valid. As a final result eigenvalue problem (4.24) again appears. The only change is in parameter $\tilde{k}$. It is now $\tilde{k} = (\bar{G} + \bar{S})k$, where is $\bar{G}$= 0.062966421. This means that periodic noise-oscillations do not disturb the phenomena of quantum δ-KR.

The classical δ-KR assuming a fully developed chaos shows a linear growth of kinetic energy (3.11). It is also well known that the quantum effects tend to suppress this diffusion due to the mechanism of dynamical localization. This is first demonstrated at δ-KR. Here, we will examine it on the basis of quantum the *atto*-KR . Thus, we suppose the wave packet initially located at 0 site in angular momentum space. We further follow its time evolution assuming (4.22). Noise-oscillations are not taken into account here. Fig.10 shows scaled kinetic energy of the wave packet calculated up to t=2000 compared with the appropriate results from quantum δ-KR . A full agreement is obtained. Suppression of classical diffusion with increasing time is present in both cases. It must be emphasized on the basis of δ-KR calculations that only for t=1 the classical and the quantum approaches give the same result. From now, for t > 1 the suppression of diffusion begins more and more. Here, we obtain at t=1 for the energy

$$E_1 \simeq \frac{\tilde{k}^2}{4}$$

assuming τ=1 . This is approximately the same result as for the classical particle obtained with the Chirikov standard map. In this way, the Chirikov standard map nevertheless appears in the quantum version of *atto*-KR . In addition, in Fig.11 the wave packet is shown in angular momentum space after t=2000 iterations. Namely, the absolute value of

$$\Psi_m^-(t) = e^{-\Omega t} u_m^-(t) \tag{4.29}$$

is shown. It is clear that the wave packet still exists on 0 site with finite probability.

V. Conclusions

The well known and researched δ-KR is an ideal version. Pulses of truly infinitesimal duration are unachievable experimentally. Thus, an approximate form of δ function is assumed. So, it has been first noted that such a version called σ-KR is quite suitable to simulate δ-KR in the limit $\frac{\bar{\varepsilon}}{T_0} \to 0$. It has already applications in molecular physics by using femtosecond laser pulses [36]. Then, σ-KR possibilities are analyzed in the here important case when $\frac{\bar{\varepsilon}}{T_0}$ is not a small parameter. A possible approximation of the APT pulses with Gaussians may be useful. After that, the APT is investigated for the first time, with respect to the application in KR. We emphasize again that $\frac{\bar{\varepsilon}}{T_0}$ in APT is surely not a small parameter. Thus, this version of KR is denoted as *atto*-KR . It seems to be the most realistic version of the KR since it takes into account the oscillations within the pulse as they appear in the experiments. The *atto*-KR is examined from both the classical and the quantum aspects. Classically, the *atto*-KR cannot be reduced to the Chirikov standard map. Therefore, a new map has been proposed. It may be useful for the experiments with classical chaos and possible applied APT. In particular, quantum *atto*-KR gives satisfactory results. Phenomena such as dynamical localization and quantum resonances appear undisturbed and they are insensitive to the periodic noise-oscillations between the pulses. Quantum *atto*-KR is also suitable for examining how the quantum effects tend to suppress the classical chaos and diffusion.

We emphasize that in Ref.[37] the atom-optics quantum KR is considered on the basis of the so-called ϵ-classical standard map. The approximation used in that paper is the same as the ones mentioned in Sec.III for σ-KR and *atto*-KR in the case when $\frac{\bar{\varepsilon}}{T_0}$ is not a small parameter. Thus, it is further shown that ϵ-classical treatment can be successfully applied to describe the dynamics of QR ratchets so far studied using purely quantum methods. It can also be an indication of the validity of the approximations distinguished in Sec.III . Nevertheless, in Ref.[38] kicks in the form of square pulse of duration $\bar{\varepsilon}$ are applied to investigate quantum resonant dynamics in finite-temperature driven gas. It should be pointed out that in that case the quantum δ-KR eigenvalue problem the same as in (4.24), appears. The difference is only in the parameter $\tilde{k}$, it is there $\tilde{k} = \frac{\bar{\varepsilon}}{T_0} k$. Then, it is important to note that this approach was adequately used in Monte Carlo simulations for investigating quantum resonances.

Moreover, it seems that the most important application of the quantum *atto*-KR can be in molecular physics for rotational excitations of diatomic molecules. Here, we give a simplified consideration of this problem from the aspect of *atto* application.

Diatomic molecules are often considered in the simple approximation as rigid rotors assuming a fixed bound length. Then, knowing equilibrium distance r_α of the two nuclei in molecule and rotational part of energy spectrum E_r^α for given state α , rotational period of molecule can be calculated based on the known expression for angular kinetic energy of classical rigid rotor as

$$T_r = \pi r_\alpha \sqrt{\frac{2\mu}{E_r^\alpha}} \quad , \tag{5.1}$$

where μ is the reduced mass of the nuclei. Thus, must be

$$\bar{\varepsilon} \ll T_r \quad , \tag{5.2}$$

assuming "kick" in the impulsive molecular alignment. Here, it should be emphasized that in the *advanced* approach with femtosecond laser pulses [39] a typical ratio $\frac{T_r}{\bar{\varepsilon}} \sim 200$ is estimated in that case therefore. Thus, supposing that the same relationship applies in the *atto* case too, the corresponding rating for T_r can be $T_r \sim 0.08$ ps . This further implies the choice of molecules and the corresponding states α . In addition, we believe that many *atto* kicks during the so determined T_r may in general improve the creation of an ensemble of aligned molecules

References

[1] F.M.Izrailev, Phys.Rep. **196**, 300 (1989)

[2] F.Haake, *Quantum signature of chaos*, Springer, Berlin (1990)

[3] S.Fishman, *Quantum localization* , in Lectures notes for the International School of Physics "Enrico Fermi" on Quantum Chaos, Varrena (1991)

[4] B.Chirikov and D.Shepelansky, Scholaropedia **3** (3), 3550 (2008)

[5] D.R.Grempel, R.E.Prange and S.Fishman, Phys.Rev. **A29**, 1639 (1984)

[6] G.Casati, Chaos **6**(3), 391 (1996)

[7] R.Scharf, J.Phys. **A22**, 4223 (1989)

[8] D.R.Mašović and A.R.Tančić, Phys.Lett. **A191**, 384 (1994)

[9] D.R.Mašović, J.Phys. **A28**, L147 (1995)

[10] L.Zhou and J.Gong, Phys.Rev. **A97**, 063603 (2018)

[11] F.L.Moore, J.C.Robinson, C.F.Bharucha, B.Sundaram and M.G.Raizen, Phys.Rev.Lett. **75**, 4598 (1995)

[12] J.Chabé, G.Lemarié, B.Grémaud, D.Delande, P.Szriftgiser and J.C.Garreau, Phys.Rev.Lett. **101**, 255702 (2009)

[13] D.H.White, S.K.Ruddell and M.D.Hoogerland, New J. Phys. **16**, 113039 (2014)

[14] M.Bitter and V.Milner, Phys.Rev.Lett. **118**, 034101 (2017)

[15] S.Zhdanovich, C.Bloomquist, J.Floß, I.Sh.Averbukh, J.W.Hepburn and V.Milner, Phys.Rev.Lett. **109**, 043003 (2012)

[16] J.Floß, S.Fishman and I.Sh.Averbukh, Phys.Rev. **A88**, 023426 (2013)

[17] K.C.Kulander, K.J.Schafer and J.L.Krause, in *Atoms in Intense Laser Fields* , edited by M.Gavrila, Academic Press, San Diego (1992)

[18] K.J.Schafer in *Strong Field Laser Physics*, edited by T.Brabec, Springer Series in Optical Sciences 134 , New York, Springer (2009)

[19] *Attosecond Physics*, edited by L.Plaja, R.Torres and A.Zair, Springer Series in Optical Sciences 177, Springer-Verlag, Berlin (2013)

[20] F.Calegari, G.Sansone, S.Stagira, G.Vozzi and M.Nisoli, J.Phys. **B49**, 062001 (2016)

[21] V.V.Strelkov, V.T.Platonenko, A.F.Sterzhantov and M.Y.Ryabikin, Usp.Fiz.Nauk **186**(5), 449 (2016) (in Russian) ; Phys.-Usp. **59**(5), 425 (2016) (in English)

[22] P.B.Corkum, Phys.Rev.Lett. **71**, 1994 (1993)

[23] P.B.Corkum, Physics Today **64**(3), 36 (2011)

[24] D.R.Mašović, Can.J.Phys. **93**, 434 (2015)

[25] D.R.Mašović, J.Mod.Opt. **64**, 1199 (2017)

[26] D.R.Mašović, M.R.Belić and J.I.Gersten, Phys.Lett. **A373**, 3289 (2009)

[27] D.R.Mašović, Chaos, Solitons and Fractals **122**, 163 (2019)

[28] P.M.Paul, E.S.Toma, P.Berger, G.Mullot, F.Augé, Ph.Balcou, H.G.Muller and P.Agostini, Science **292**(5522), 1689 (2001)

[29] K.J.Schafer, M.B.Gaarde, A.Heinrich, J.Biegert and U.Keller, Phys.Rev.Lett. **92**, 023003 (2004)

[30] C.Figueira de Morisson Faria and P.Salières, Laser Phys. **17**, 390 (2007)

[31] P.Antoine, A.L'Huillier and M.Lewenstein, Phys.Rev.Lett. **77**, 1234 (1996)

[32] L.E.Reichl, *The Transition to Chaos*, Springer-Verlag, New York (1992)

[33] J.P.Cryan, P.H.Bucksbaum and R.N.Coffee, Phys.Rev. **A80**, 063412 (2009)

[34] L.S.Schulman, *Techniques and Applications of Path Integration*, Wiley, New York (1981)

[35] D.L.Shepelansky, Phys.Rev.Lett. **56**, 677 (1986)

[36] M.Bitter and V.Milner, Phys.Rev. **A95**, 013401 (2017)

[37] M.Sadgrove and S.Wimberger, New J.Phys. **11**, 083027 (2009)

[38] B.T.Beswick, I.G.Hughes, S.A.Gardiner, H.P.A.G.Astier, M.F.Andersen and B.Daszuta, Phys.Rev. **A94**, 063604 (2016)

[39] S.Fleischer, Y.Khodorkovsky, Y.Prior and I.Sh.Averbukh, New J.Phys. **11**, 105039 (2009)

Figure captions

Fig.1

Electric field $E_h(t-t_0)/E_h^0$ corresponding to APT , where t is given in attoseconds.

Fig.2

Map given by (3.7) and (3.8) is shown for the value of parameter $\bar{K} = 50$.

Fig.3

Map given by (3.7) and (3.8) is shown for the value of parameter $\bar{K} = 100$.

Fig.4

Map given by (3.7) and (3.8) is shown for the value of parameter $\bar{K} = 150$.

Fig.5

Map given by (3.7) and (3.8) is shown for the value of parameter $\bar{K} = 500$.

Fig.6

Scaled (dividing by 100) rotational energy for $\bar{K}= 500$, where n is dimensionless time .

Fig.7

Dynamical localization in angular momentum space for τ=1 $\tilde{k}$=30 .
Results $\ln(\mathrm{mod}(\ u_m^+))$ as a function of m for the appropriate even state
are obtained by solving (4.24) . The estimated localization length is $\sim$ 150
assuming pseudo-random transfer matrix approach or $\sim$ 11 as in Ref.[5] .

Fig.8

Dynamical localization in angular momentum space for τ=1 $\tilde{k}$=30 .
Results $\ln(\mathrm{mod}(\ v_m^-))$ as a function of m for the appropriate odd state
are obtained by solving (4.25) .

Fig.9

Quantum resonance in angular momentum space for $\tau = 2\pi$ $\tilde{k}$=30 .

Fig.10

Scaled (dividing by 100) kinetic energy in time, corresponding

a.) red quantum δ-KR , k =30

b.) black quantum *atto*-KR , $\tilde{k}$ =30

for τ= 1 .

Fig.11

mod($\Psi_m^-(t)$) in angular momentum space for t=6000

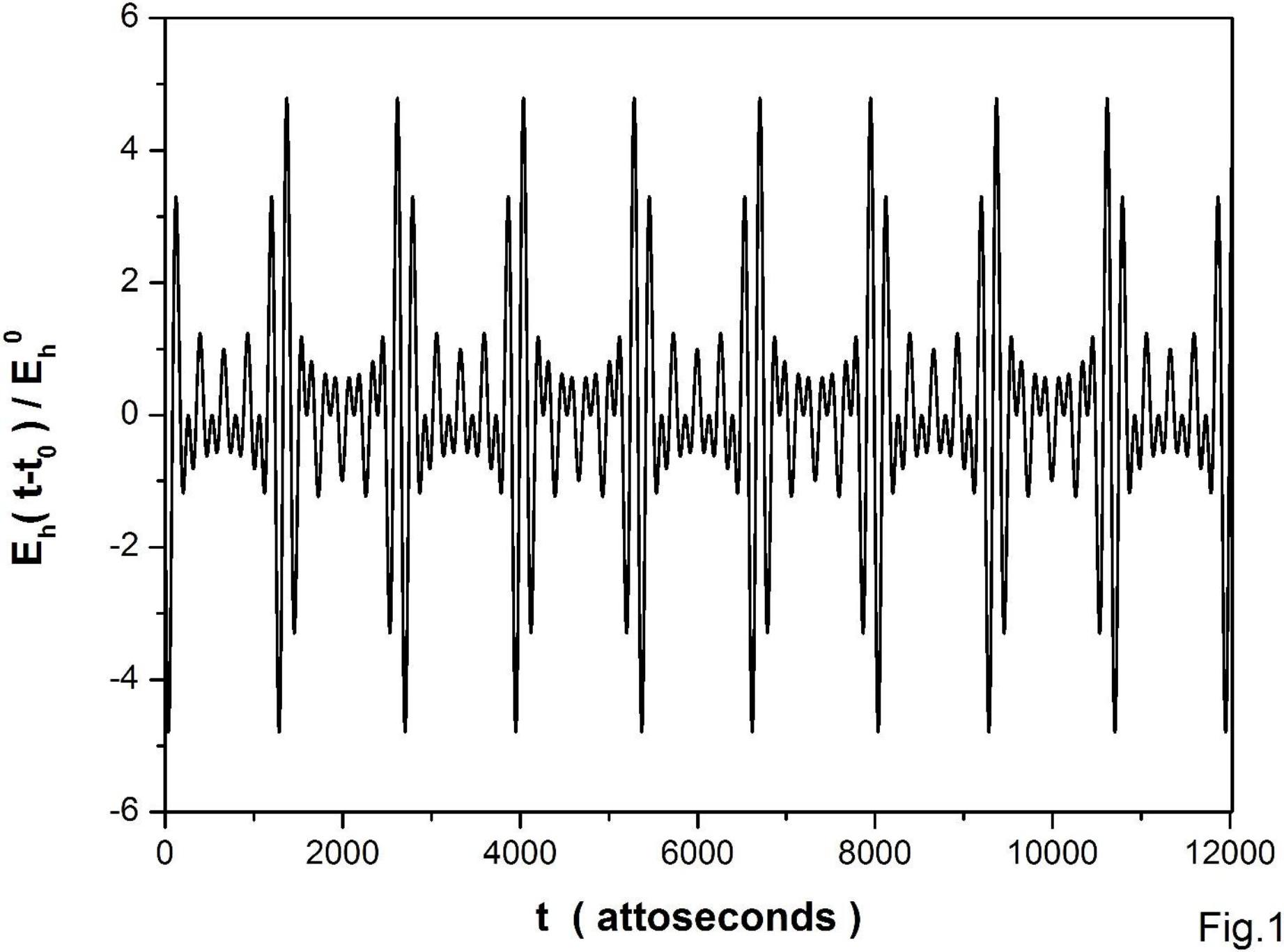
6
4
2
0
-2
-4
-6
0
2000
4000
6000
8000
10000
12000
$E_h(t-t_0) / E_h^0$
t (attoseconds)

Fig.1

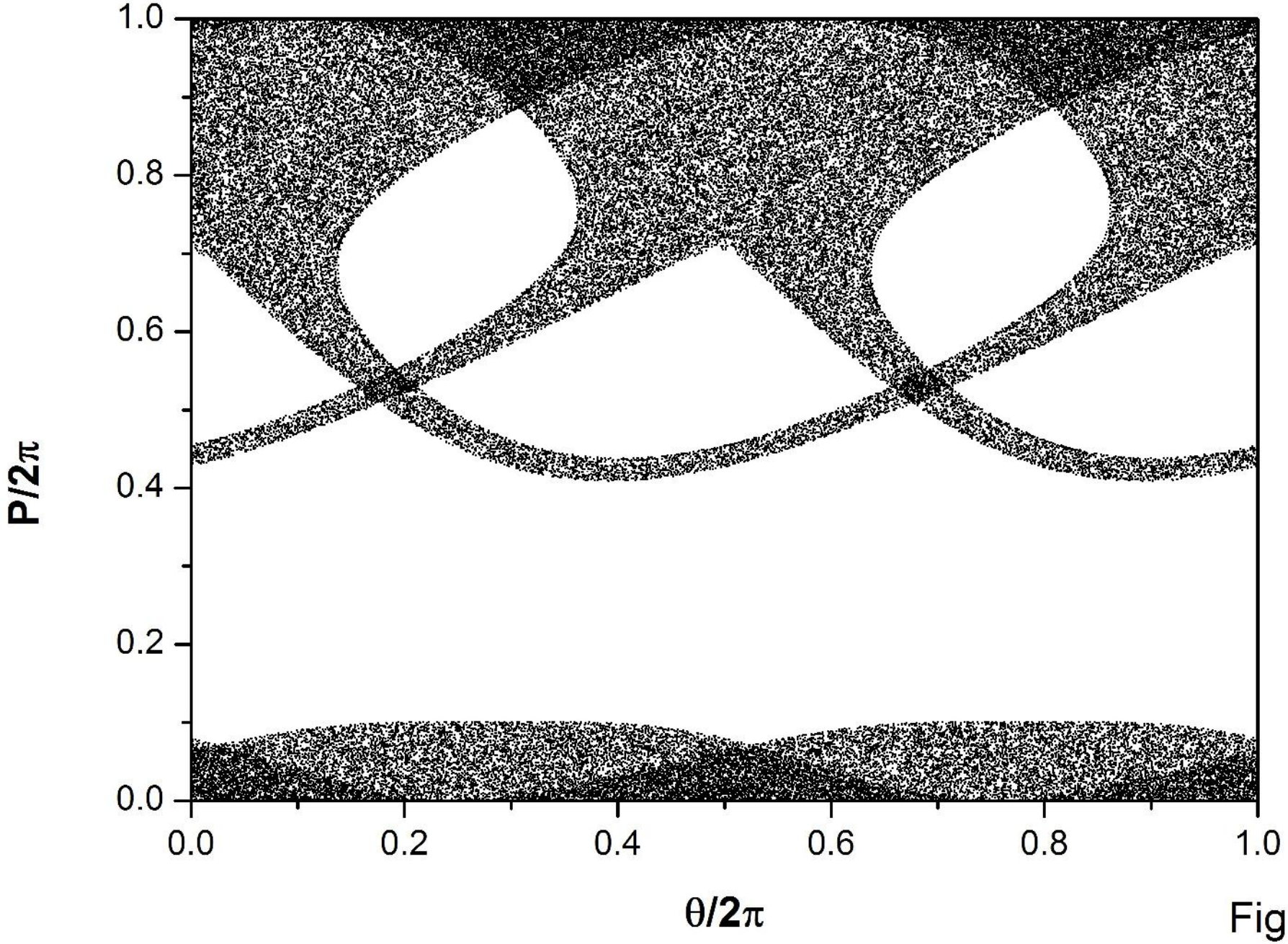

Fig.2

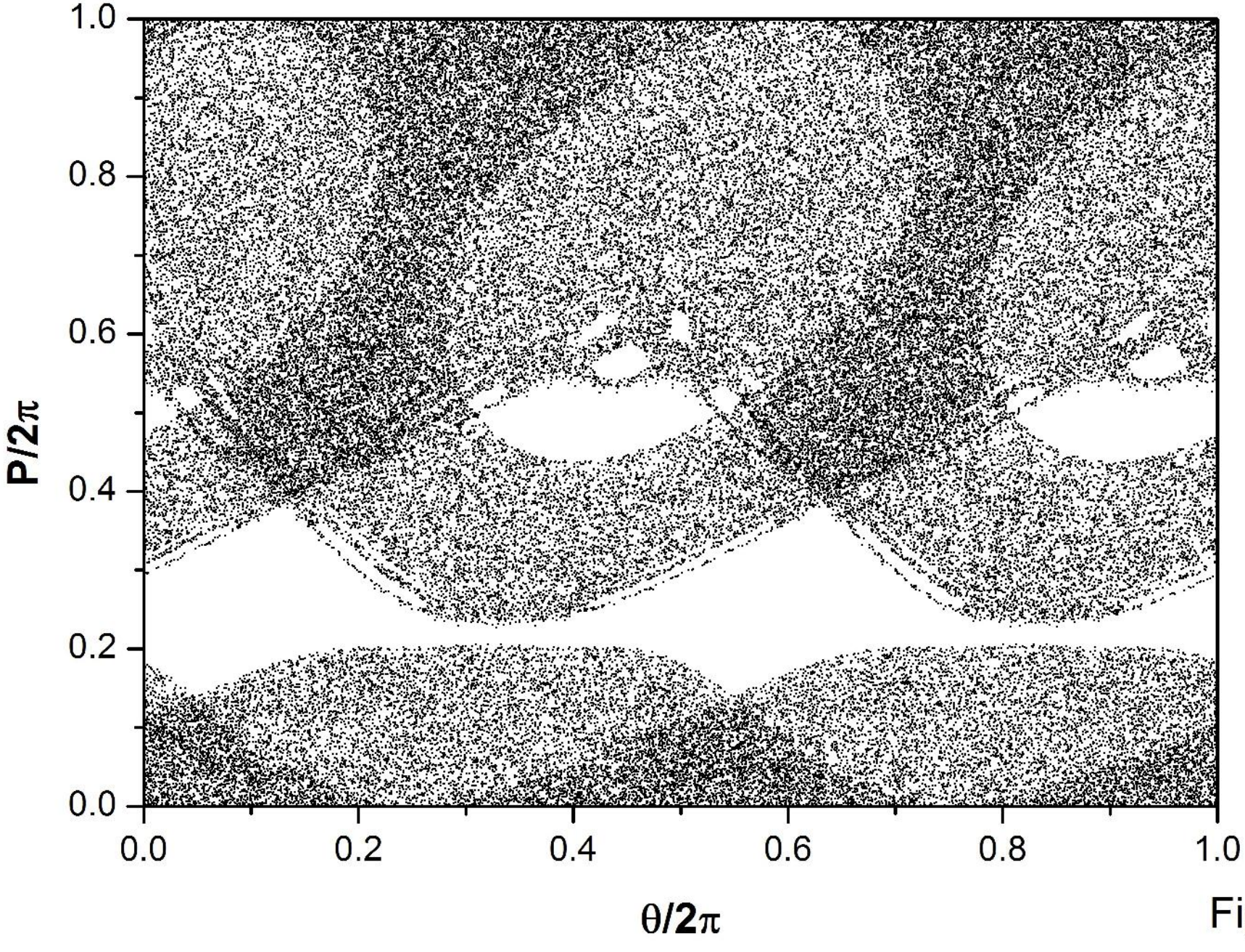

Fig.3

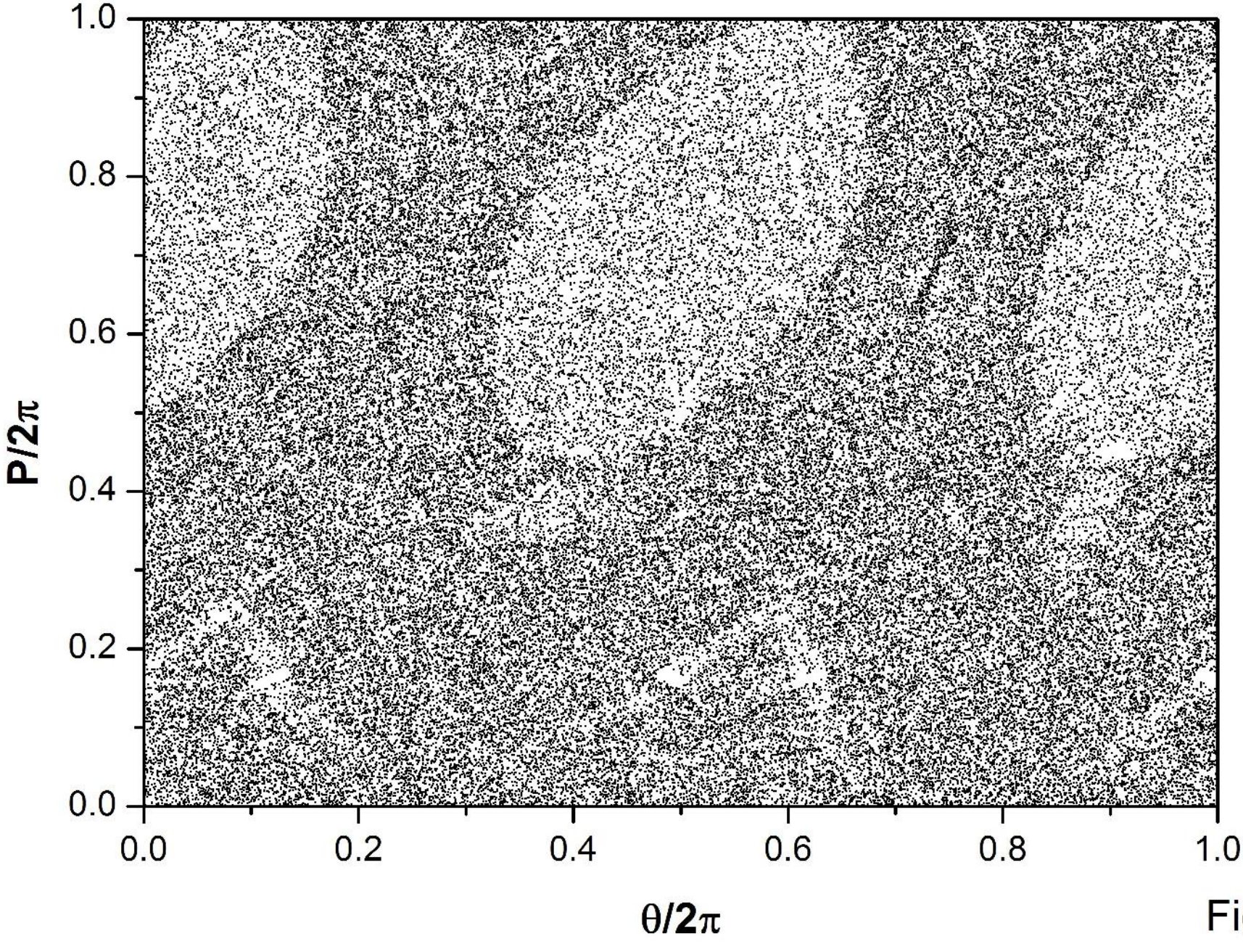

Fig.4

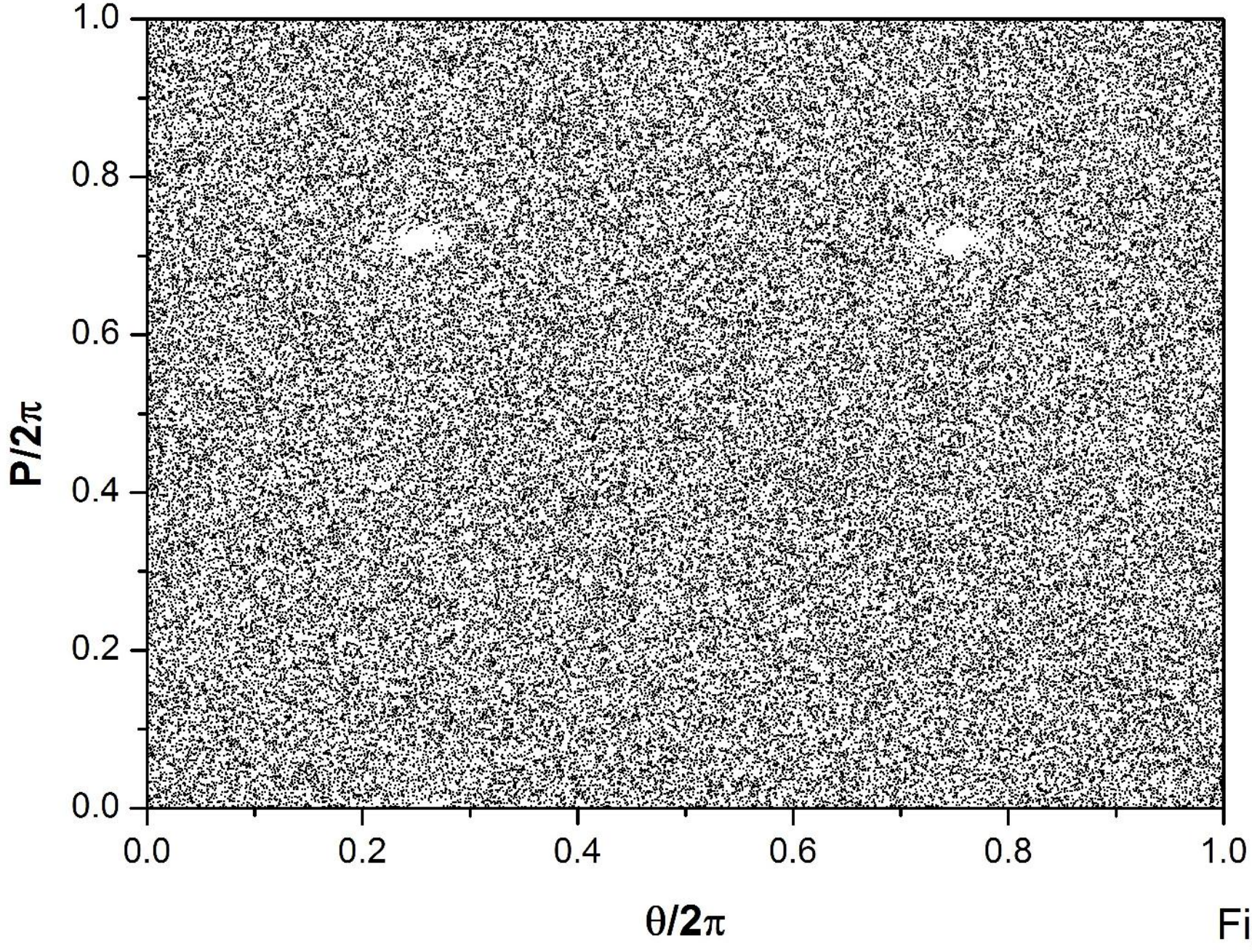

Fig.5

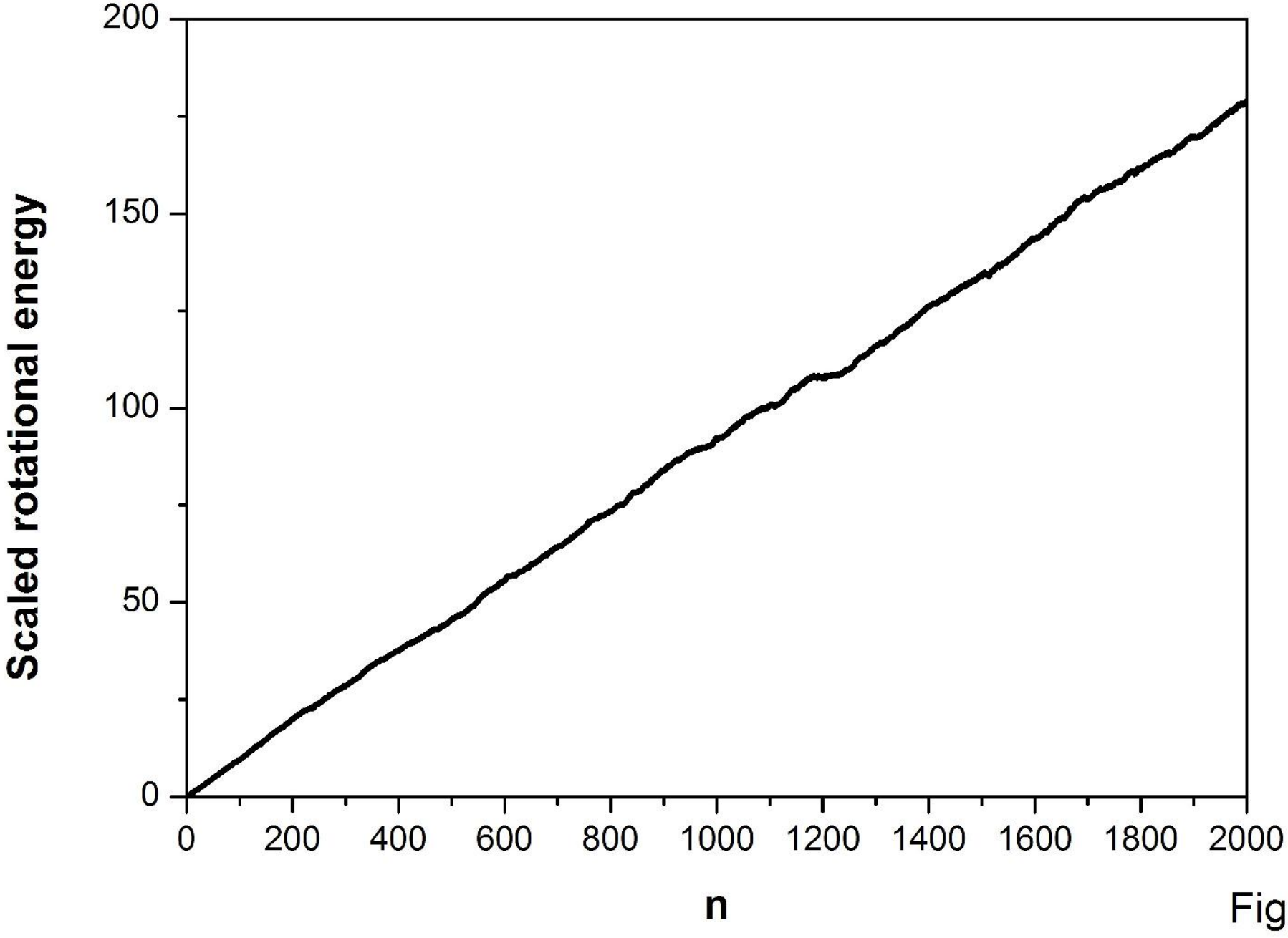
Scaled rotational energy
200
150
100
50
0
0
200
400
600
800
1000
1200
1400
1600
1800
2000
n

Fig.6

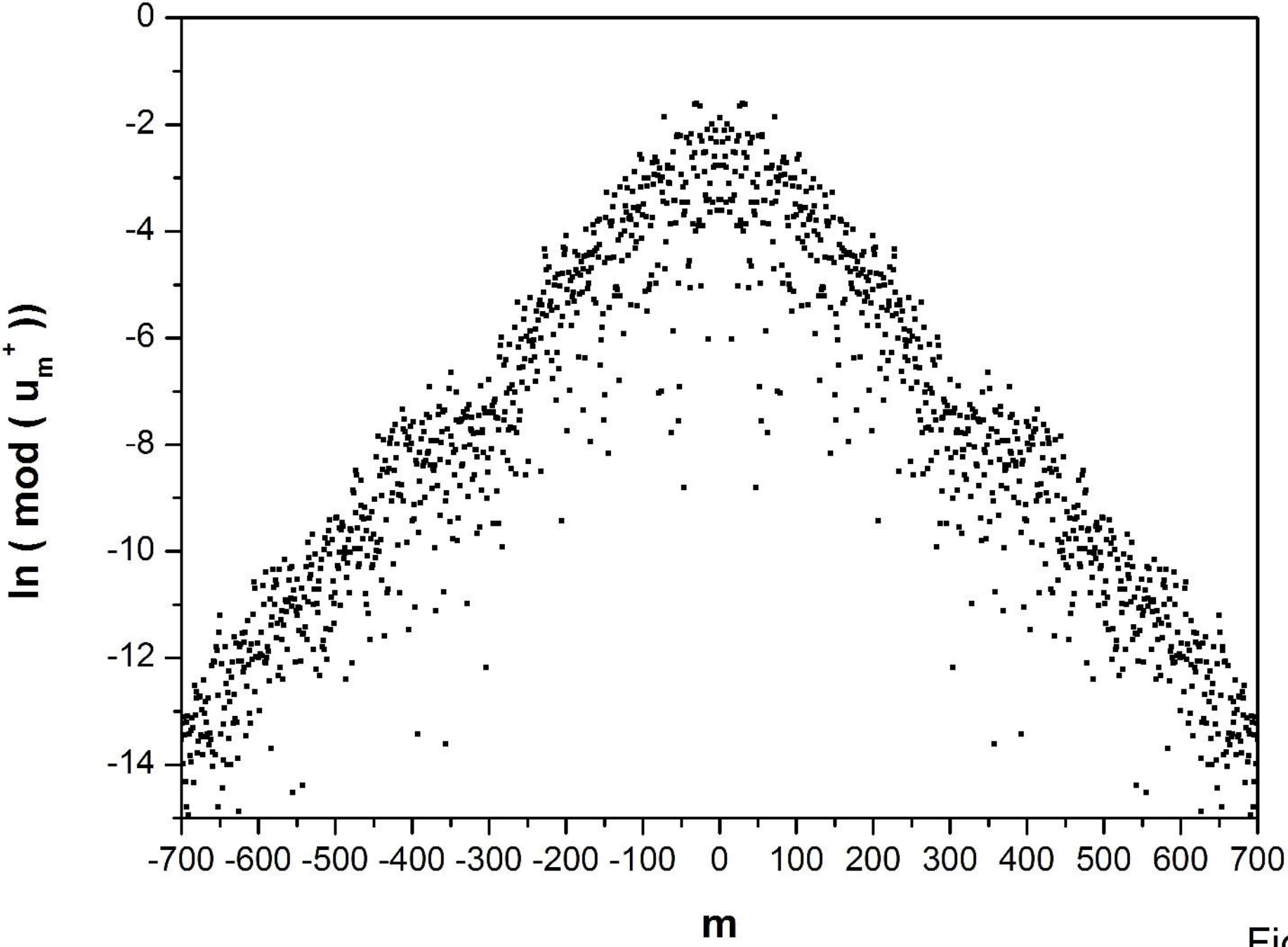
0
-2
-4
-6
-8
-10
-12
-14
ln (mod (u_m^+))
-700 -600 -500 -400 -300 -200 -100 0 100 200 300 400 500 600 700
m

Fig.7

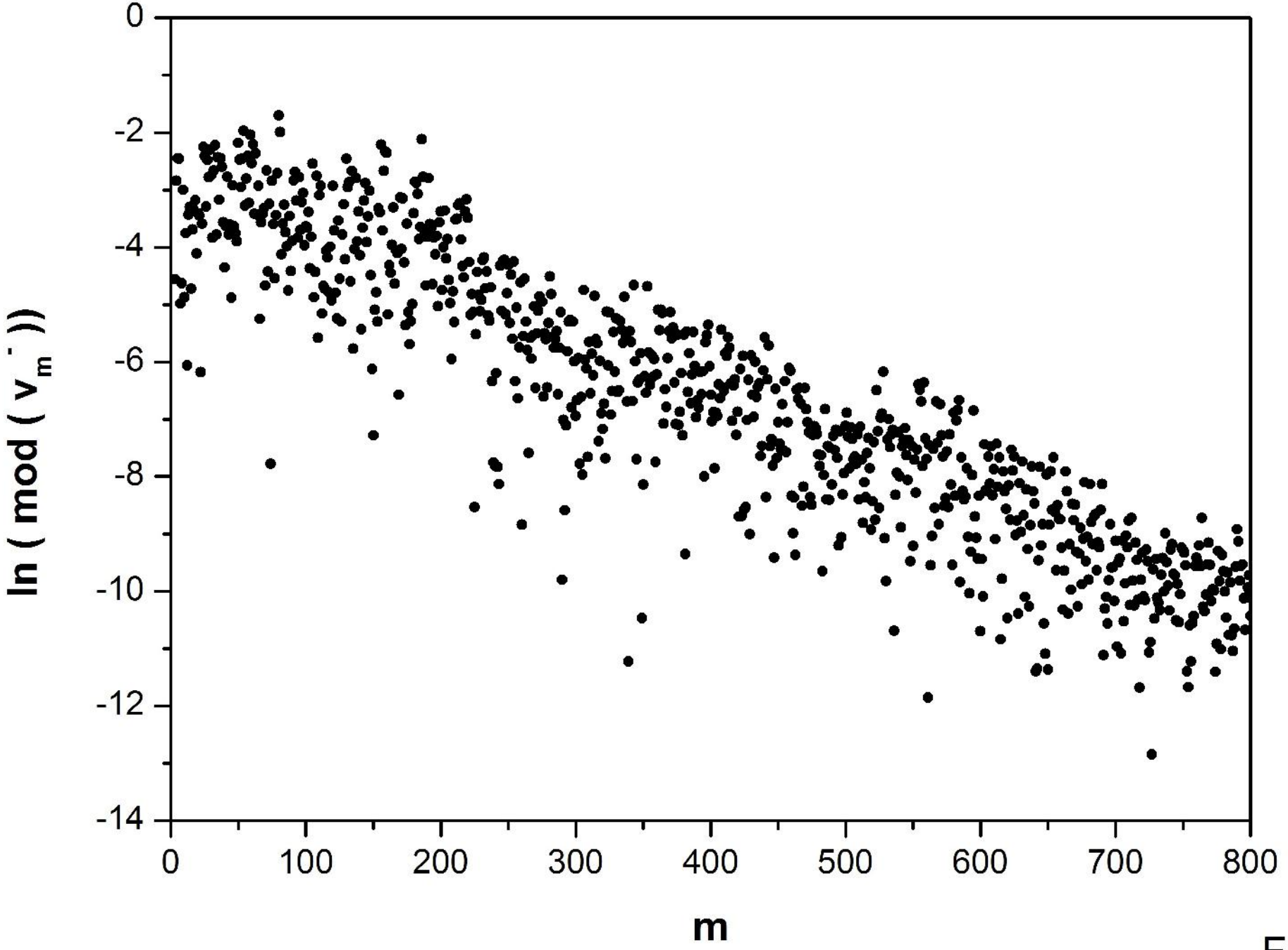

Fig.8

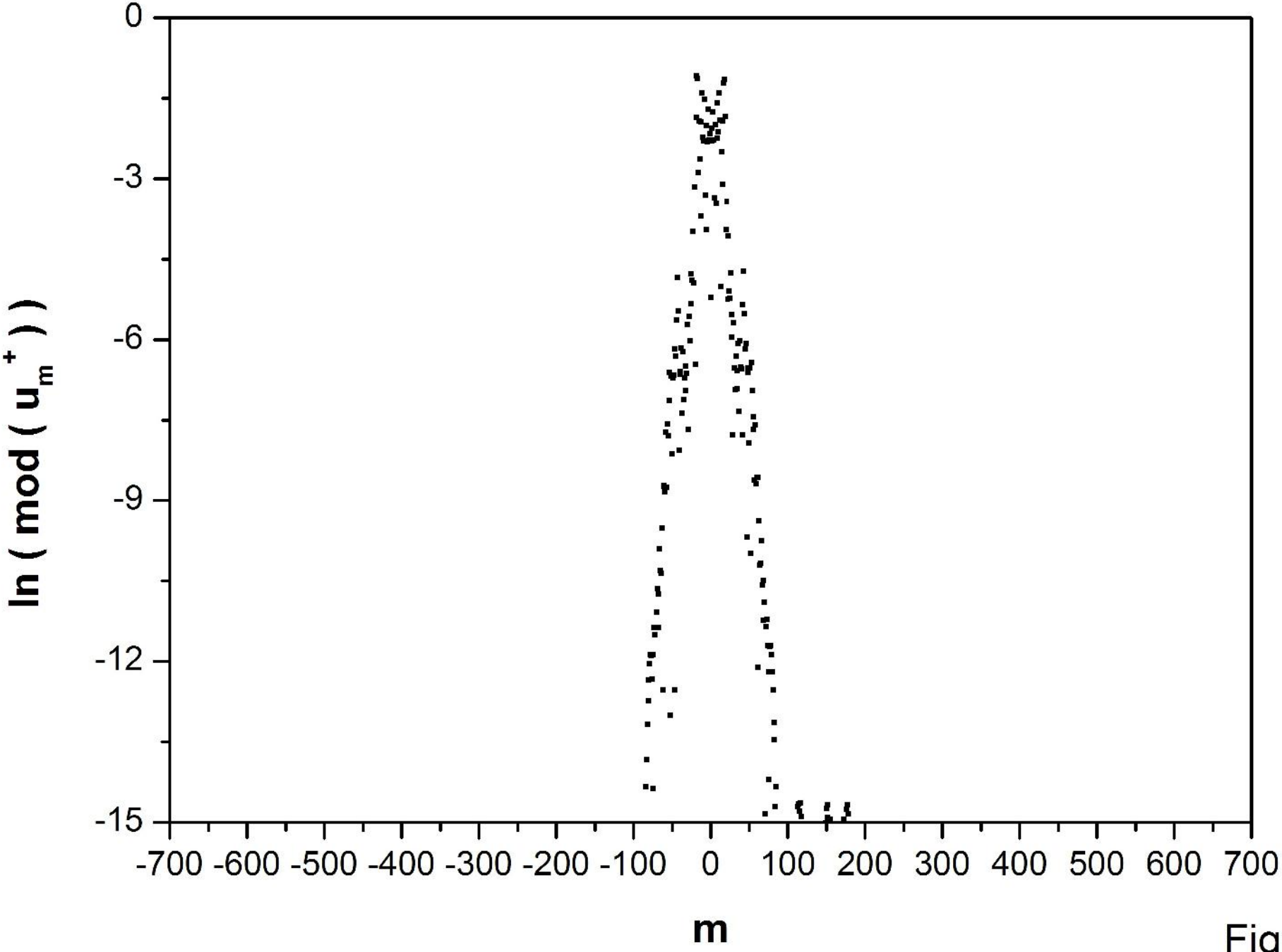
0
-3
-6
-9
-12
-15
ln (mod (u_m^+))
-700 -600 -500 -400 -300 -200 -100 0 100 200 300 400 500 600 700
m

Fig.9

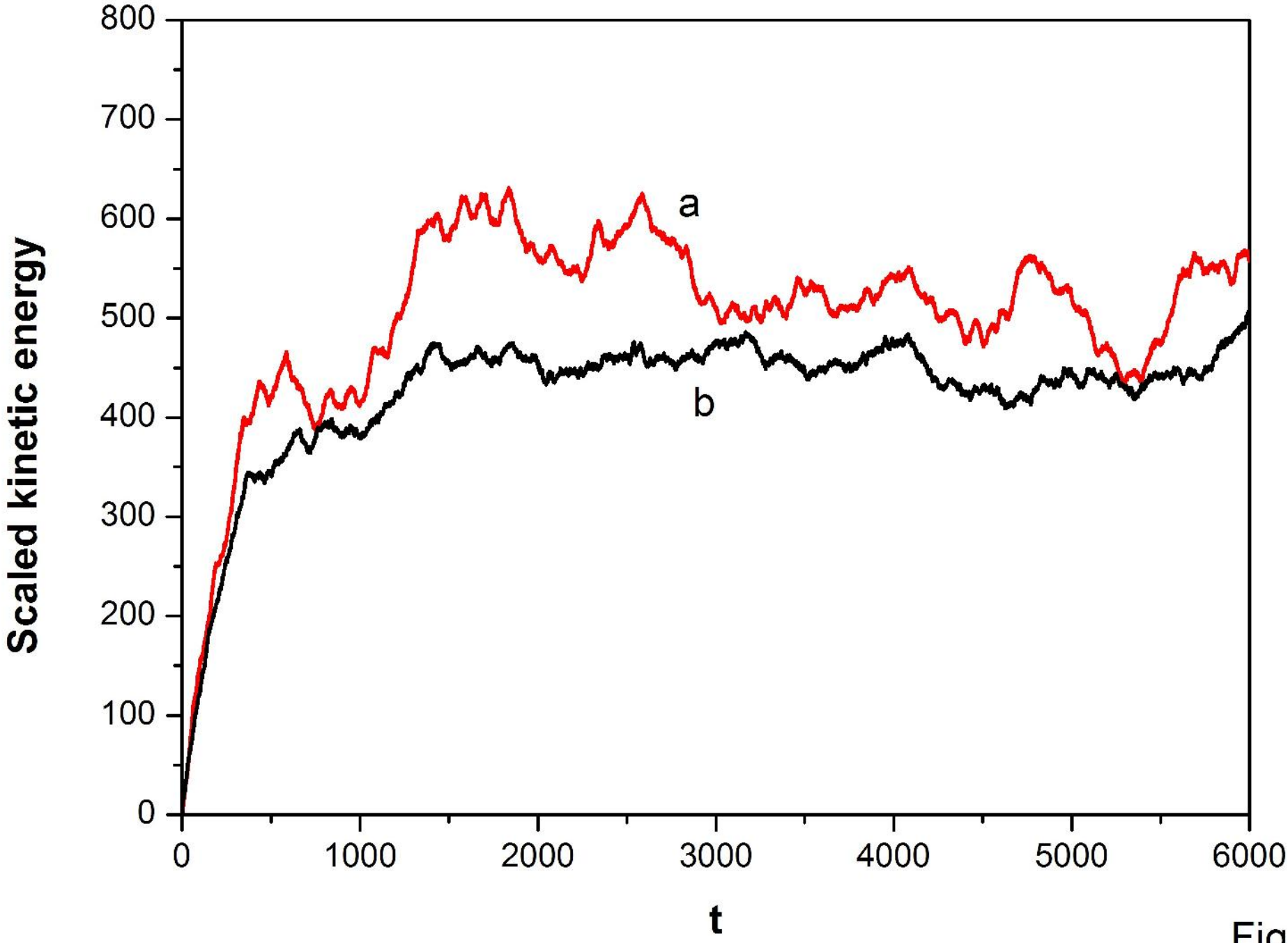
Scaled kinetic energy
800
700
600
500
400
300
200
100
0
0
1000
2000
3000
4000
5000
6000
t
a
b

Fig.10

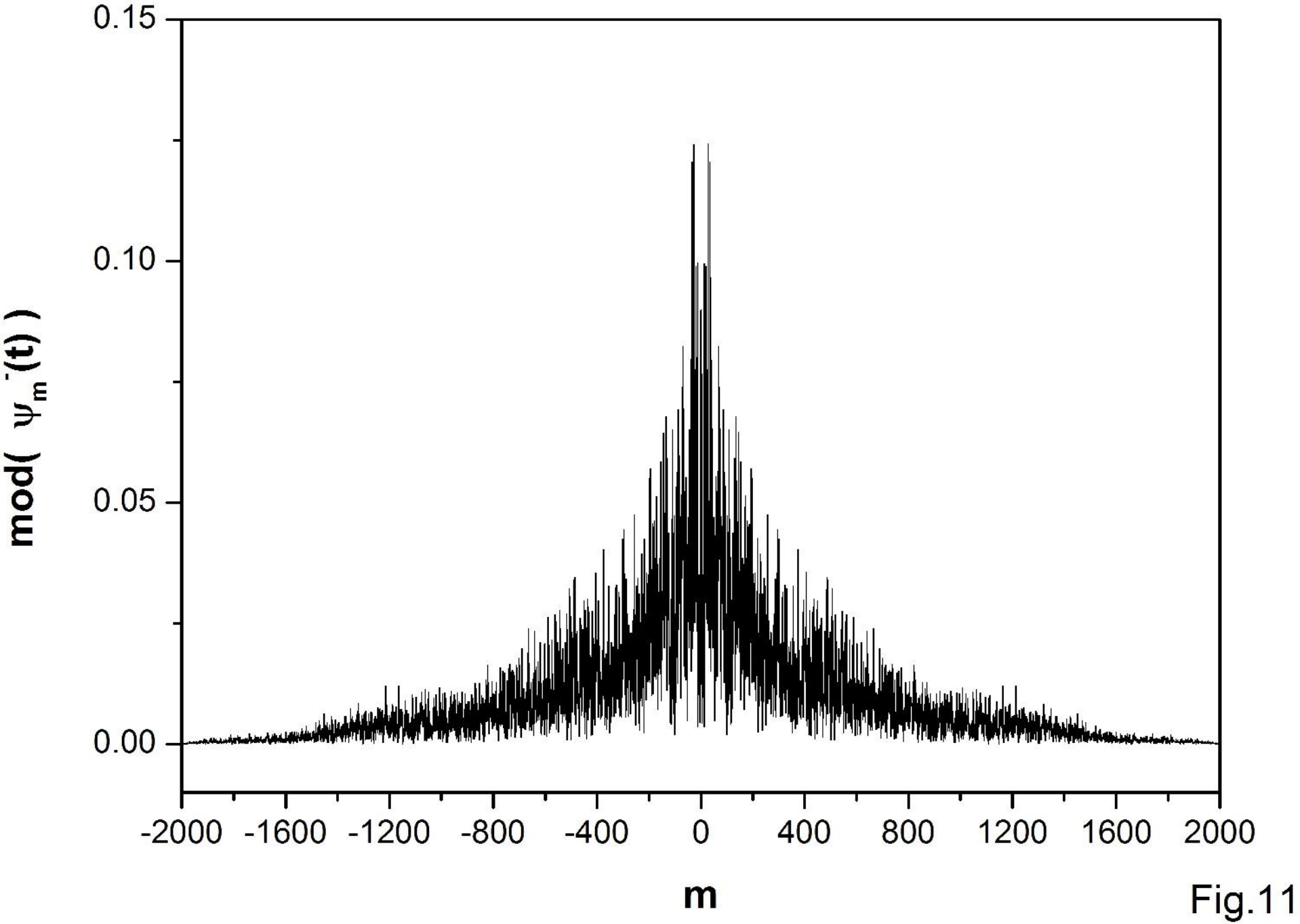
0.15
0.10
0.05
0.00
mod(ψm(t))
-2000
-1600
-1200
-800
-400
0
400
800
1200
1600
2000
m

Fig.11